Journal of Cerebral Blood Flow & Metabolism (2010) 30, 1712–1720
© 2010 ISCBFM All rights reserved 0271-678X/10 $32.00
www.jcbfm.com

Combined contrast-enhanced ultrasound and rt-PA treatment is safe and improves impaired microcirculation after reperfusion of middle cerebral artery occlusion

Max Nedelmann[1,2], Nouha Ritschel[3], Simone Doenges[1,2], Alexander C Langheinrich[4], Till Acker[5], Peter Reuter[1,2], Mesut Yeniguen[1], Jan Pukropski[2], Manfred Kaps[1], Clemens Mueller[2], Georg Bachmann[2] and Tibo Gerriets[1,2]

[1]*Department of Neurology, Justus Liebig University, Giessen, Germany;* [2]*Department of Experimental Neurology, Justus Liebig University, Giessen and Kerckhoff Clinic, Bad Nauheim, Germany;* [3]*Max-Planck-Institute for Heart and Lung Research, Bad Nauheim, Germany;* [4]*Department of Radiology, Justus Liebig University, Giessen, Germany;* [5]*Institute of Neuropathology, Justus Liebig University, Giessen, Germany*

In monitoring of recanalization and in sonothrombolysis, contrast-enhanced ultrasound (CEUS) is applied in extended time protocols. As extended use may increase the probability of unwanted effects, careful safety evaluation is required. We investigated the safety profile and beneficial effects of CEUS in a reperfusion model. Wistar rats were subjected to filament occlusion of the right middle cerebral artery (MCA). Reperfusion was established after 90 minutes, followed by recombinant tissue-type plasminogen activator (rt-PA) treatment and randomization to additional CEUS (contrast agent: SonoVue; 60 minutes). Blinded outcome evaluation consisted of magnetic resonance imaging (MRI), neurologic assessment, and histology and, in separate experiments, quantitative 3D nano-computed tomography (CT) angiography (900 nm³ voxel size). Nano-CT revealed severely compromised microcirculation in untreated animals after MCA reperfusion. The rt-PA partially improved hemispheric perfusion. Impairment was completely reversed in animals receiving rt-PA and CEUS. This combination was more effective than treatment with either CEUS without rt-PA or rt-PA and ultrasound or ultrasound alone. In MRI experiments, CEUS and rt-PA treatment resulted in a significantly reduced ischemic lesion volume and edema formation. No unwanted effects were detected on MRI, histology, and intracranial temperature assessment. This study shows that CEUS and rt-PA is safe in the situation of reperfusion and displays beneficial effects on the level of the microvasculature.
Journal of Cerebral Blood Flow & Metabolism (2010) **30,** 1712–1720; doi:10.1038/jcbfm.2010.82; published online 9 June 2010

Keywords: microbubbles; microcirculation; reperfusion; sonothrombolysis; stroke

Introduction

Transcranial color-coded duplex sonography (TCCS) is a well-established bedside method for rapid evaluation of intracranial hemodynamics in acute stroke. It provides functional and prognostic information valuable for individual patient management (Allendoerfer *et al*, 2006; Nedelmann *et al*, 2009; Perren *et al*, 2006; Wunderlich *et al*, 2007). Next to diagnostic applications, randomized clinical studies suggest therapeutic efficacy of ultrasound on recanalization of acute cerebral artery occlusion in terms of an acceleration of fibrinolysis with recombinant tissue-type plasminogen activator (rt-PA) (Alexandrov *et al*, 2004; Eggers *et al*, 2008). Echo contrast agents may further improve treatment efficacy (Molina *et al*, 2006; Perren *et al*, 2008).

These monitoring and therapeutic approaches require extended insonation periods. Although ultrasound is regarded as being safe, extended monitoring and therapeutic strategies are subject of discussion as prolonged exposure times of ischemic tissue may potentially increase the risk of side effect occurrence. It is unclear, whether repeated use of contrast agents may further increase the likelihood of adverse effects.

Correspondence: Dr M Nedelmann, Department of Neurology, Justus Liebig University, Am Steg 14, 35392 Giessen, Germany.
E-mail: max.nedelmann@neuro.med.uni-giessen.de
This study was supported by the Pitzer Foundation, Bad Nauheim, Germany. The nano-CT is supported in part by the German research foundation (DFG; 162/291-1 FUGG).
Received 16 December 2009; revised 22 April 2010; accepted 19 May 2010; published online 9 June 2010

A recent animal study showed safe applicability of contrast-enhanced ultrasound (CEUS) monitoring after permanent MCA occlusion (Fatar *et al*, 2008). However, reperfusion into the ischemic and abnormally permeable vascular bed leads to particular vulnerability toward secondary hemorrhage (Henning *et al*, 2008; Thomalla *et al*, 2007). Therefore, safety aspects of CEUS have to be regarded specifically for this situation.

Successful recanalization of large arteries may result in persisting hypoperfusion of the ischemic territory due to microcirculatory obstruction (Dawson *et al*, 1997). There is still uncertainty about involved factors (Dirnagl *et al*, 1994). Okada *et al* identified fibrin deposits as one possible cause (Okada *et al*, 1994). This raises the issue whether microcirculatory obstruction is accessible to sonothrombolytic treatment.

This study was designed to evaluate the safety profile and potential treatment effects of microbubble-enhanced sonothrombolysis during reperfusion after MCA occlusion in a rat model. Outcome evaluation consisted of magnetic resonance imaging (MRI), histology, and functional evaluation. For evaluation of the microvascular perfusion territories, a quantitative analysis of the vasculature was performed in a separate series of experiments, using high-resolution 3D micro- and nano-computed tomography (micro- and nano-CT). Micro- and nano-CT's technical feasibility to visualize intracerebral arteries has been shown earlier (Langheinrich *et al*, 2007, 2009).

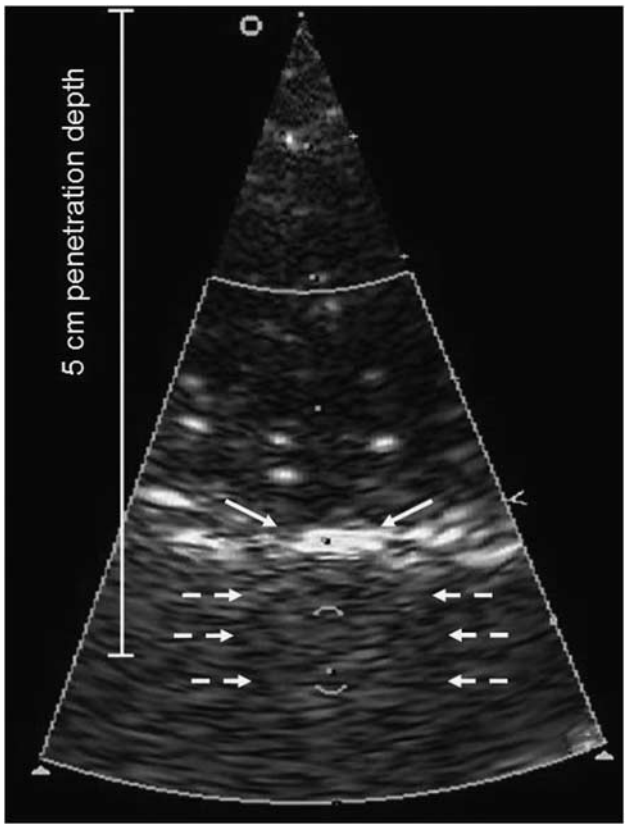

Figure 1 Ultrasound setup. Distance from probe surface to skull was 4 cm, the sample volume placed in midbrain, resulting in a penetration depth of 5 cm. Continuous arrows denote reflection at rat skull and dotted arrows denote lateral boundary of skull.

Materials and methods

Animal Preparation

A total of 84 male Wistar rats (body weight 311 ± 20.0 g; Harlan Winkelmann, Germany) were used in the study. Procedures were in accordance with the German animal protection legislation and approved by the regional ethics committee (AzB2/189).

Anesthesia was started with 5% isoflurane inhalation for 2 minutes and maintained with 2% to 3% at 0.5 L/min. Rectal temperature was maintained at 36.5°C to 37.0°C. Blood gases, oxygen saturation, acid-base state, pH, and hemoglobin were measured before surgery, after reperfusion, and after treatment. Right hemispheric cerebral ischemia was induced as described earlier (Nedelmann *et al*, 2008). In brief, a 4-0 silicone-coated nylon suture was advanced 20 to 25 mm beyond the carotid bifurcation until mild resistance indicated the tip being lodged in the anterior cerebral artery, thus blocking blood flow to the MCA. Reperfusion was induced by removing the suture after 90 minutes.

Experimental Setup

Treatment period started 10 minutes after established reperfusion. The rt-PA (Actilyse, Boehringer Ingelheim, Germany) was given intravenously at 10 mg/kg body weight, 10% as bolus followed by a 1-hour infusion.

The TCCS was applied in parallel to rt-PA. A 1 to 3 MHz diagnostic sector probe was used with B-mode and color-Doppler functions switched on (Sonos 7500; Philips Ultrasound Systems, Bothell, WA, USA). The probe was set at maximum output, resulting in a mechanical index of 1.7, and positioned 4 cm above the shaved scalp (Figure 1). The distance between probe and scalp was bridged with a gel-filled spacer. The sound beam was aimed to expose the entire brain with spectral Doppler sample volume of 0.57 cm placed within the midbrain. The control groups had the probe placed but switched off.

Sulfur hexafluoride microbubbles were used as echo contrast agent (SonoVue; Bracco Research, Plan-Les-Ouates, Switzerland). Animals received 10 μL of commercial standard solution (8 μL microbubbles per mL solution), administered intravenously at four time points (0, 15, 30, and 45 minutes from onset of treatment period), diluted in 90 μL of isotonic saline before injection. This dose was calculated by comparing blood volume of humans with rats. Control animals received the same amount of saline.

Substudy 1: Quantitative Assessment of the Cerebral Vasculature

This study was performed in 21 animals. The MCA reperfusion was as described earlier. Animals were treated

in seven different groups with a treatment period of 60 minutes: Control group 1: euthanization directly after reperfusion; control group 2: euthanization 60 minutes after reperfusion; group 3: treatment with rt-PA; group 4: treatment with combined CEUS and rt-PA; group 5: treatment with ultrasound alone; group 6: treatment with CEUS without rt-PA; group 7: treatment with combined ultrasound and rt-PA (without contrast enhancer).

For preparation of CT scanning, animals were transcardially perfused with isotonic saline, until the venous effluent was free of blood. The aortic arch was prepared and ligations were placed on the aorta (proximal and distal of brain supplying arteries), the subclavian arteries, and the external carotid arteries. A measure of 10 mL of a lead-containing radiopaque polymer (Microfil, Flow-Tech, Carver, MA, USA) were infused through aortic puncture.

All brains were scanned using micro-CT (SkyScan1072_80 kV; Belgium). The X-ray system is based on a microfocus tube (20 to 80 kVp, 0 to 100 μA) reaching a minimum spot size of 8 μm at 8 W generating projection images irradiating X-rays in cone-beam geometry. This system has been described in detail before (Langheinrich *et al*, 2004). The resulting 3D images were displayed using Analyze 8.0 (Biomedical Imaging Resource, Mayo Clinic, Rochester, MN, USA). The micro-CT scanner was configured to a 12 μm side dimension of the cubic voxels.

For detailed analysis of the brain microvessels, samples were cut with a side length of 4 mm and rescanned using the nano-CT (SkyScan, Kontich, Belgium). The microfocus X-ray source is a pumped-type (open type) source with an LaB6 cathode. The electron beam is focused by two electromagnetic lenses onto the surface of an X-ray target (Au), containing a thin tungsten film plated on the surface of the beryllium window, producing X-ray emission reaching a minimum spot size of <400 nm. Small-angle scattering enhances object details down to 150 nm isotropic voxels size. The X-ray detector consists of a 12-bit digital, water-cooled CCD high-resolution (1280×1024 pixel) camera with fiber optic 3.7:1 coupling to an X-ray scintillator and digital frame grabber. Samples were positioned on a computer controlled rotation stage and scanned 180° around the vertical axis in rotation steps of 0.25 degrees at 40 kVp. Acquisition time for each view was 2.4 seconds. The total contrast agent volume (= total vascular volume; mm^3) of nano-CT images was measured in the right and left hemisphere using the Analyze software package. The total contrast agent volume represents the sum of all pixels marked as contrast agent after thresholding. Therefore, contrast perfused animals were used. For determination of the vascular volume, rectangular regions of interest (side length, 3 mm at 8 bit) were established manually inside the region of interest.

Substudy 2: Safety Analysis and Treatment Effects on Basis of Functional Outcome, Magnetic Resonance Imaging, and Histology

Operation procedures were as described earlier. Animals were randomized into two groups ($n = 25$ each). One group received rt-PA treatment after reperfusion, the other group had CEUS treatment in addition to rt-PA.

Functional evaluation: After 24 hours, the animals were functionally evaluated by use of the previously validated NeuroScore (Nedelmann *et al*, 2007). This score tests for motor, coordinative, and sensory items. Overall functional impairment is scored from 0 (no impairment) to 90 (maximum impairment). Each item scores 0 (no impairment) or 10 (impairment), except for spontaneous walking (0: normal gait; 5: drifting/circling; 10: unable to walk on ground). Used items were as follows: inability to fully extend left forelimb; instability to lateral push from right; tail suspension test. In this test, animals were gently lifted by the tail and impairment was assumed when animals flexed their body to the left and remained in that position in three consecutive attempts; walking on ground (see above); whisker movements on left side (present or absent); consciousness (normal or no reactions to stimuli); hearing (normal or no reaction to clapping of hands); sensory (normal or no reaction to left-sided touch or prick); and left-sided hemianopia (normal or repeatedly absent reaction to visual stimuli approaching from left).

Thereafter, MRI was performed. The animals were then deeply anesthetized, euthanized, and the brains removed for histology.

Magnetic resonance imaging evaluation: The animals were fixed in a body restrainer with tooth-bar and a cone-shaped head holder and were placed in an MRI spectrometer (Bruker PharmaScan 70/16, 7.0 T, 16 cm; Ettlingen, Germany). Respiratory rate was monitored with a pressure probe placed between the restrainer and the animal's thorax. Temperature was monitored using a rectal probe. Body temperature was maintained at 37°C by a thermostatically regulated and feedback controlled water flow system, consisting of a pump-driven cylindrical tube system surrounding the animal's body while sparing the head holder. The head holder was then placed into a custom-designed linear polarized volume resonator (diameter 60 mm) and tuned and matched manually.

To map the apparent diffusion coefficient of water, diffusion-weighted images were acquired by use of a fat suppressing echo planar imaging (EPI) sequence. An increase of the intracellular volume due to cell swelling as a cause of cytotoxic edema results in an almost immediate apparent diffusion coefficient decline (Gerriets *et al*, 2004). A volume shim with a volume selective double spin echo sequence (repetition time (TR) = 1 second, echo time (TE) = 30 milliseconds, voxel size $10 \times 8 \times 15\ mm^3$) was performed before the acquisition of the first diffusion series to optimize imaging quality. The achieved full width at half maximum of the water line was about 25 to 35 Hz. Six contiguous coronal slices with a thickness of 2 mm were collected with a field of view of $32 \times 32\ mm^2$ and a matrix size of 128×128 (TR = 3003 milliseconds, TE = 38.6 milliseconds, number of excitations (NEX) = 4). A fourfold segmentation was used to reduce image artifacts caused by local field inhomogeneity. Five sets of coronal images were recorded for quantitative determination of apparent diffusion coefficient, with equidistant diffusion gradient values of 10, 40, 70, 100, and 130 mT/m and with a diffusion gradient duration (δ) of 9 milliseconds and a gradient separation time (Δ) of 15 milliseconds. This

results in five *b*-values of 6.96, 111.3, 340.8, 695.6, and 1175.5 s/mm^2. The acquisition time for each EPI sequence was 4.5 minutes.

T2 relaxation time was mapped using a Carr Purcell Meiboom Gill spin echo sequence. This sequence is highly sensitive to the number of protons within the tissue and thus allows mapping and quantification of the brain water content and vasogenic edema formation (Gerriets *et al*, 2004). Measurement was performed in cortical and subcortical regions of interest of the ischemic area on each slice. The difference between the ischemic and the unaffected contralateral hemisphere was calculated. Hemorrhage was evaluated by T2* imaging. Six slices with a thickness of 2 mm were acquired with a field of view of 37×37 mm^2 and a matrix size of 512×256 (TR = 3833.5 milliseconds, 90° excitation and 180° rephasing pulses, NEX = 1). Twelve echoes were collected, starting with TE = 18 milliseconds (step size ΔTE = 18 milliseconds), resulting in a range from 18 to 216 milliseconds. Acquisition time for each Carr Purcell Meiboom Gill sequence was 16 minutes and 21 seconds.

Computer-aided planimetric assessment of the lesion and hemispheric volumes was performed using image analysis software (Image J 1.37v; National Institutes of Health, USA). Ischemic lesion volume was assessed by diffusion weighted and T2 imaging. Lesion volume is expressed in percent of the hemisphere (% hemispheric lesion volume = %HLV).

Histology: The brains were fixed in 4% formalin and embedded in paraffin. A measure of 4 μm sections through the frontal, parietal, and occipital cortex and brain stem were cut, mounted on SuperFrost microscope slides (Menzel-Glaeser, Germany), dried for 45 minutes at 70°C and incubated for 24 hours at 37°C. Sections were rehydrated in solutions with decreasing ethanol concentration and stained with hematoxylinand eosin.

Substudy 3: Temperature Evaluation

Temperature effects of transcranial insonation were assessed in 12 animals. All animals received CEUS in combination with rt-PA. Operation procedures were as described earlier. In six animals, a temperature probe was placed through a small occipital burr hole into the ischemic territory. Six further animals had the probe placed within the nonischemic contralateral hemisphere. Temperature was determined throughout the treatment period.

Statistical Analysis

Outcome evaluation was performed by experienced investigators blinded for group assignment. Data are presented as mean ± s.d. Analyses were performed using SPSS 15.0. After confirmation of normal distribution, infarct volume, edema formation, and functional outcome between the two experimental groups were compared using two-sided *t*-test. Nano-CT statistical analysis was performed using JMP 6.0. Vascular volume fraction was analyzed using unpaired *t*-test and one-way analysis of variance. $P < 0.05$ was considered significant in all analyses.

Results

All animals survived treatment and the observation period, except for one animal that died during surgery (subarachnoid hemorrhage after advancing the suture). After anesthesia, all animals recovered to normal vigilance. The physiological blood parameters, body temperature, and body weight of the animals did not differ between the experimental groups and remained within the normal physiological range throughout the surgical and treatment procedure.

Substudy 1: 3D Micro- and Nano-Computed Tomography Evaluation

Results are shown in Figures 2–4. Figures 2 and 3 show micro- and nano-CT results of exemplary animals, Figure 4 gives results of the determination of the vascular volume. A significantly reduced vascular volume fraction was found in nontreated animals after reperfusion, as compared with the nonoccluded left hemisphere ($P < 0.001$). Treatment with rt-PA resulted in partial improvement, whereas animals treated with rt-PA in combination with CEUS (contrast-enhanced sonothrombolysis) showed reversal of flow obstruction with similar vascular volume fractions between both hemispheres (Figure 4A). Compared with these results, treatment with ultrasound alone did not show any benefit compared with the nontreated controls. Treatment with CEUS (without rt-PA) and treatment with rt-PA in combination with ultrasound (without contrast enhancer) resulted in partial improvement associated with a still statistically significant impairment compared with the left hemisphere (Figure 4B), thus being inferior to the treatment effects seen after treatment with rt-PA and CEUS.

Substudy 2: Magnetic Resonance Imaging Evaluation, Functional Outcome, and Histology

The ischemic lesion volume was smaller in CEUS and rt-PA-treated animals, compared with controls receiving rt-PA monotherapy (Table 1). This difference was statistically significant ($P < 0.05$) on the basis of both diffusion weighted (24.1% ± 9.5% versus 30.6% ± 11.6%) and T2 evaluation (22.0% ± 11.5% versus 29.5% ± 11.8%). Exemplary MRI is shown in Figures 5C and 5D. T2 relaxation time determination of edema formation gave lower values in animals exposed to CEUS (22.2 ± 9.9; controls: 26.1 ± 7.4; $P < 0.05$; Table 1).

The NeuroScore did not indicate significant differences with regard to functional outcome between CEUS and rt-PA treated and sham insonated animals ($P = 0.20$; Table 1).

T2* imaging and histology revealed signs of intracerebral hemorrhage in 1 of 25 animals treated with CEUS and rt-PA and in none of the animals in

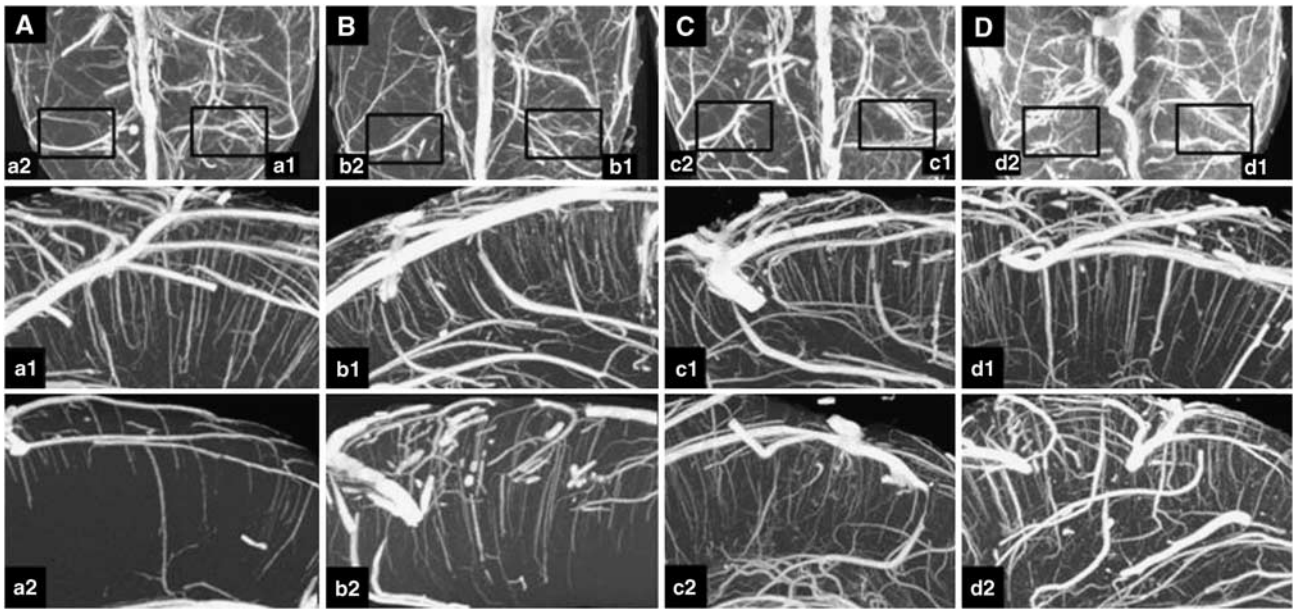

Figure 2 Maximum-intensity projection (MIP) using micro- and nano-computed tomography (CT) in exemplary animals. (**A**–**D**) (Upper row) Axial view on micro-CT scans. For nano-CT analysis, regions of interest (boxes) were cut and rescanned. MIPs from nano-CT in coronal view are shown in (a1/2–d1/2): preparation directly after reperfusion (**A**, a1/2); 60 minutes after reperfusion (**B**, b1/2); after recombinant tissue-type plasminogen activator (rt-PA) (**C**, c1/2), and after rt-PA and contrast-enhanced ultrasound (CEUS) (**D**, d1/2). The nonoccluded left hemisphere is presented from a1 to d1. Persisting impairment of microcirculation (a2/b2) is partially improved after rt-PA treatment (c2) and completely reversed with rt-PA and CEUS (d2).

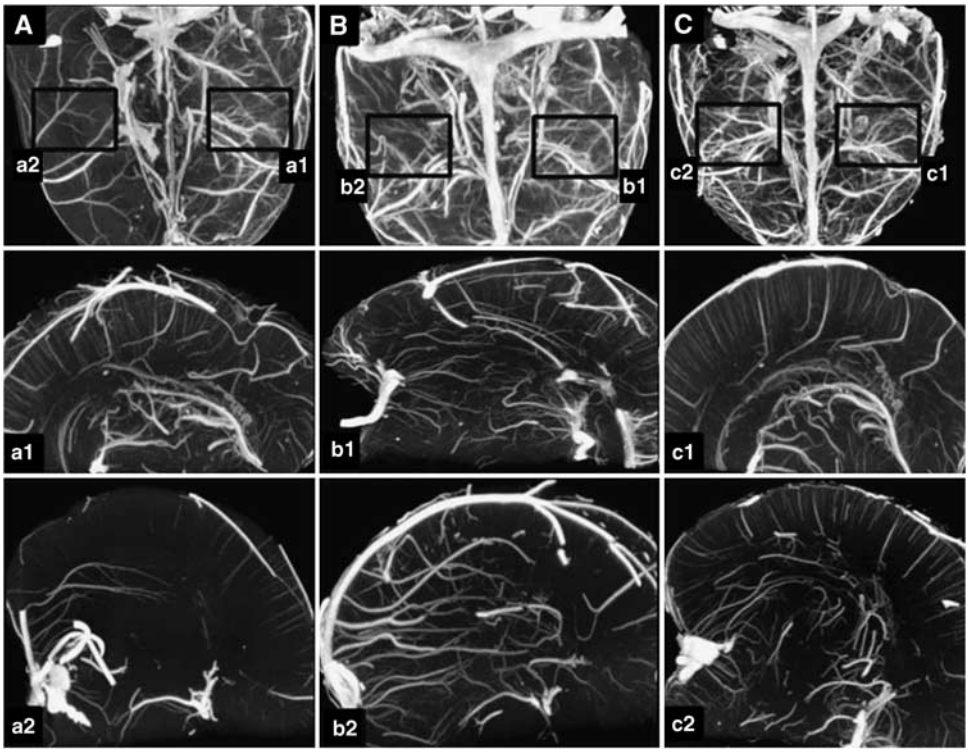

Figure 3 Maximum-intensity projection (MIP) using micro-computed tomography (CT) (**A**–**C**) and nano-CT (a1/2–c1/2) in exemplary animals after treatment with ultrasound alone (**A**, a1/2), contrast-enhanced ultrasound (CEUS) without recombinant tissue-type plasminogen activator (rt-PA) (**B**, b1/2), and rt-PA with ultrasound (without contrast enhancer) (**C**, c1/2). The nonoccluded hemisphere is presented from a1 to c1. The figure illustrates persisting impairment of microcirculation after ultrasound treatment (a2) and partial improvement after CEUS treatment and treatment with rt-PA and ultrasound (b2/c2).

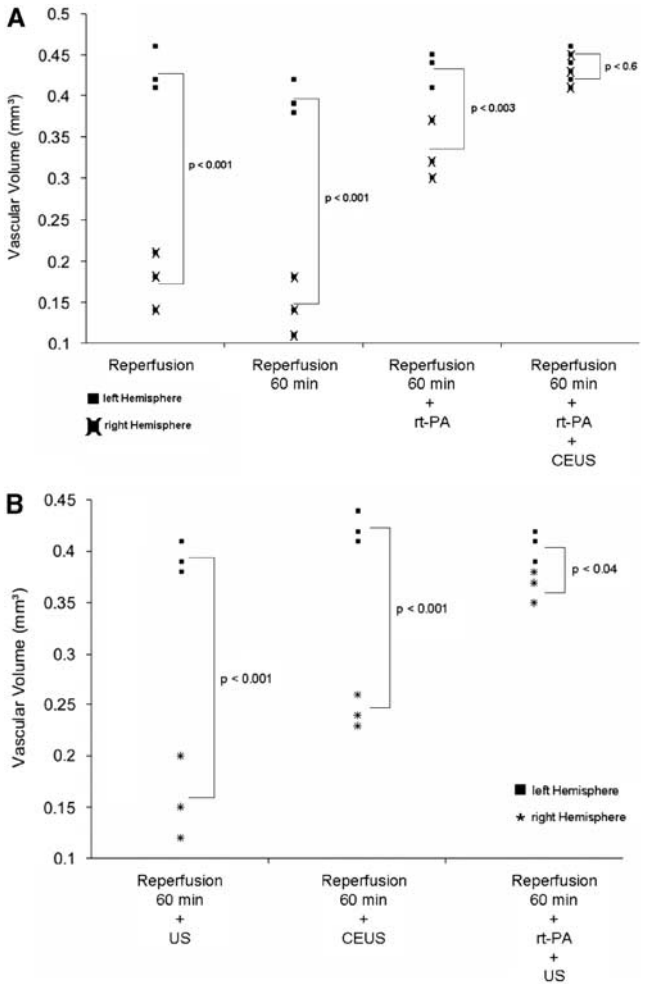

Figure 4 Nano-computed tomography quantification. (**A**) Significant differences in the total vascular volume fraction between the right and left hemisphere are found in animals after reperfusion and animals treated with recombinant tissue-type plasminogen activator (rt-PA). No significant differences are present after treatment with rt-PA and contrast-enhanced ultrasound (CEUS). (**B**) No treatment effects were seen in animals treated with ultrasound alone. The CEUS without rt-PA and ultrasound with rt-PA (without contrast enhancer) showed partial improvement inferior to the effects seen after treatment with rt-PA and CEUS.

Table 1 MRI and functional outcome 24 hours after treatment of animals in substudy 2

	rt-PA+CEUS	*rt-PA only*
Infarct volume (%HLV)	24.1 ± 9.5*	30.6 ± 11.6
T2RT (milliseconds)	22.2 ± 9.9*	26.1 ± 7.4
NeuroScore	41.4 ± 13.4	45.4 ± 7.5

CEUS, contrast-enhanced color-duplex ultrasonography; %HLV, hemispheric lesion volume on basis of diffusion weighted imaging; MRI, magnetic resonance imaging; rt-PA, recombinant tissue-type plasminogen activator; T2RT, T2 relaxation time as indicator of edema formation.
Values are presented as mean ± s.d.
*$P < 0.05$.

the rt-PA group. The detected hemorrhage was located within the ischemic territory, was small and not space occupying, and was not associated with neurologic deterioration. Corresponding histology and MRI findings are shown in Figures 5A and 5B.

Substudy 3: Temperature Evaluation

Intracranial temperature during treatment with CEUS and rt-PA was assessed in 12 animals, six animals had the probe placed within the ischemic territory, and six animals in the nonischemic contralateral hemisphere. Compared with baseline, there were no significant changes of intracerebral temperature throughout the treatment period (Figure 6). Maximum temperature increase of single values was 0.4°C within the ischemic territory, and 0.9°C within the contralateral hemisphere.

Discussion

This study evaluated therapeutic and safety aspects of CEUS after reperfusion of MCA occlusion. Our nano-CT study (substudy 1) shows occlusion of small vessels down to the capillary level in untreated animals, albeit established MCA reperfusion. We chose the CT approach, as high-resolution 3D micro- and nano-CT imaging permits analysis of the vasculature in microscopic detail (Langheinrich *et al*, 2007). In comparison, MRI has major limitations in the spatial resolution needed to visualize and quantify changes in the microvasculature (Pfeuffer *et al*, 2002).

Compared with untreated controls, administration of rt-PA resulted in partial improvement of perfusion. Impairment was completely reversed after microbubble-enhanced sonothrombolysis (Figure 4). The results of our MRI study (substudy 2) show that this treatment effect on the microvasculature results in a statistically significant reduction of the ischemic lesion volume, as compared with rt-PA monotherapy (Table 1).

Earlier animal studies have shown that 'no reflow' within the microvascular compartment is an important condition after MCA occlusion that promotes infarct development (Dawson *et al*, 1997; Okada *et al*, 1994). Okada *et al* showed that local formation of fibrin contributes to microvascular obstruction (Okada *et al*, 1994), which may explain the—partial—treatment effect we found after administration of rt-PA. Further improvement of this effect by microbubble-enhanced ultrasound is in line with experimental data showing that the efficacy of rt-PA on fibrin-rich clots can be enhanced in combination with ultrasound (Saguchi *et al*, 2008).

It has been shown that postischemic hypoperfusion is preceded by early hyperemia—not lasting longer than 15 minutes—as a consequence of

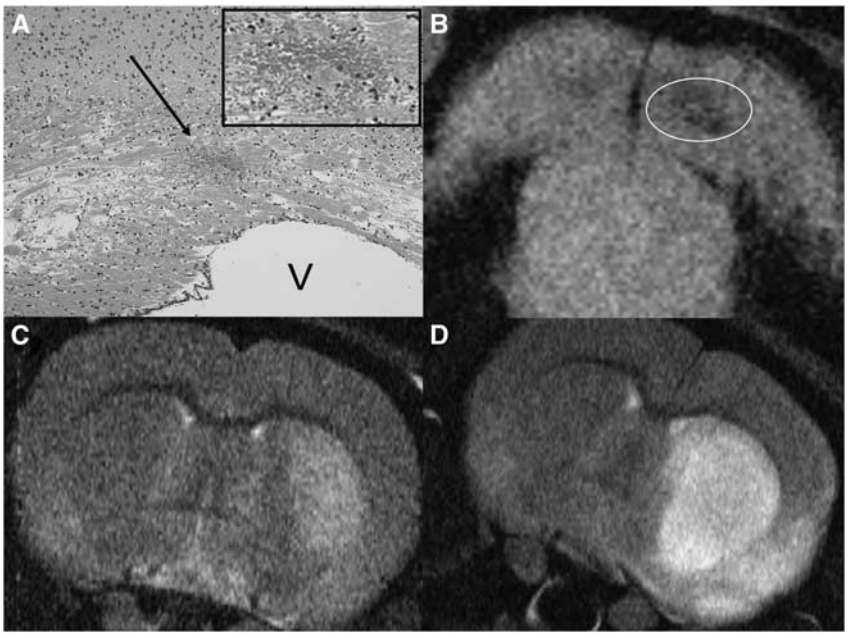

Figure 5 Hemorrhagic transformation was found in one animal treated with contrast-enhanced ultrasound (CEUS) and recombinant tissue-type plasminogen activator (rt-PA). (**A**) Hematoxylin and eosin staining of hemorrhage (arrow). Magnification of hemorrhage is shown in the upper right corner (frame). (**B**) Corresponding T2* magnetic resonance imaging of hemorrhage (circle). The bottom pictures show examples of ischemic demarcation after treatment with CEUS and rt-PA (**C**) and after treatment with rt-PA (**D**). V, ventricle.

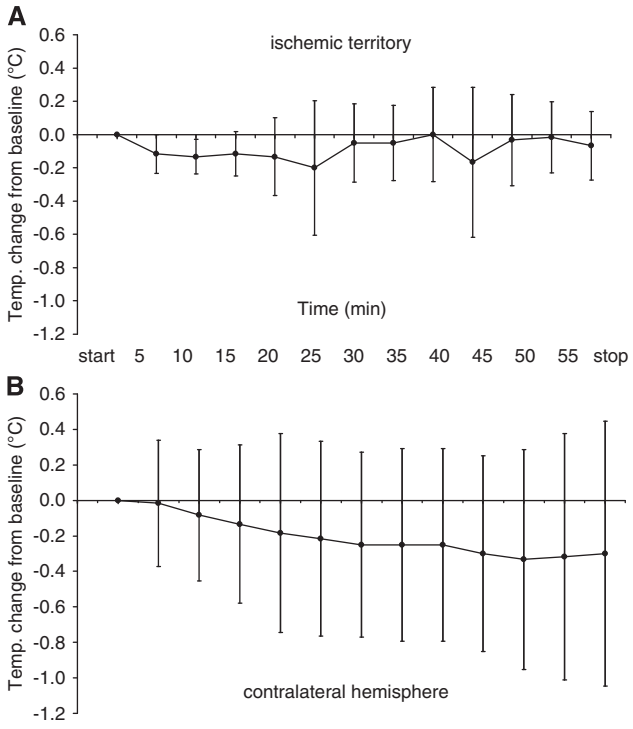

Figure 6 Intracerebral temperature changes during 1 hour insonation with contrast-enhanced transcranial color-coded duplex sonography. All animals additionally received recombinant tissue-type plasminogen activator. The temperature probe was placed into the territory of the right reperfused middle cerebral artery (**A**, $n = 6$) and in the nonischemic contralateral hemisphere (**B**, $n = 6$). Maximum temperature increase of single values was 0.4°C in (**A**) and 0.9°C in (**B**).

reperfusion into a maximally vasodilated arterial bed (Dirnagl *et al*, 1994; Todd *et al*, 1986). In this context, it has been suggested that recovery of vascular smooth muscle tone may contribute to subsequent hypoperfusion (Todd *et al*, 1986). Animal studies have shown that ultrasound application can significantly improve tissue perfusion in rabbit muscle and myocardial ischemia after fixed arterial occlusion (Siegel *et al*, 2004; Suchkova *et al*, 2002). The effect is inhibited by administration of a nitric oxide synthase inhibitor, suggesting an nitric oxide (NO)-dependent mechanism of ultrasound-induced vasodilation. These effects have not yet been investigated in the cerebral vasculature. In summary, the mechanisms leading to persisting occlusion of the microvascular compartment after reperfusion are not well understood and merit further research activities. Future studies should also address whether vasodilatory effects of transcranial ultrasound may have influenced the treatment effects we observed in our study.

The primary aim of our study was to investigate the combined effect of ultrasound, microbubbles, and rt-PA on improvement of microcirculation. Indeed, the most prominent treatment effect was seen for this combination. In our nano-CT substudy, we additionally evaluated other modalities of therapeutic ultrasound. No effects were found after treatment with ultrasound alone. Compared with this, the combination of ultrasound and contrast agent (without rt-PA) resulted in a moderate improvement of the vascular volume of the affected hemisphere. As this treatment option may be of interest in patients with contraindication against

rt-PA, further studies should address this application in more detail. Most importantly, our results show that contrast-enhanced sonothrombolysis may provide more benefit than the conventional combination of rt-PA with unenhanced ultrasound. This finding supports the approach to focus on contrast-enhanced sonothrombolysis in the planning of future multicenter studies.

Another issue is the mechanism by which bubbles exposed to ultrasound can achieve optimal treatment effects. Our experimental setup does not allow the investigation of bubble dynamics, that is, whether destruction or oscillation of microbubbles in the sound field (stable cavitations) are most beneficial. An earlier *in vitro* study suggested that stable cavitation activity may result in strongest treatment effects (Datta *et al*, 2008). Further investigations need to address this interesting field of research.

The second part of this study is related to safety. By means of functional evaluation, MRI, histology, and temperature assessment, we could not detect any adverse effects related to CEUS as an add-on measure to rt-PA.

In the routine setting, contrast-enhanced TCCS is accepted as a safe method for evaluation of the intracranial arteries in acute stroke (Nedelmann *et al*, 2009). To prevent potential side effects, application generally follows the ALARA principle (as low as reasonably achievable). In a series of patients who had an intracranial pressure/temperature probe implanted, no heating effects were found during routine ultrasound examination (Schlosser *et al*, 2009). Because of the prolonged insonation time protocols, therapeutic applications have to be regarded separately. In addition, induction of cavitation phenomena by repeated dosing of microbubbles may further contribute to local heating. In our study, the temperature probes were placed within the ischemic territory, as this area may be specifically prone to heating due to impaired perfusion. We additionally measured intracerebral temperature in the contralateral hemisphere, to test for temperature effects in areas where presumably the contrast agent is more available over time. Relevant temperature effects were not detected. This is in contrast to the results of Nakagawa *et al*, who found temperature elevation up to 2.41°C during prolonged 2 MHz Doppler monitoring in healthy rabbits (Nakagawa *et al*, 2007). This difference may be explained by the experimental setup, as the probe was placed directly above the skull and thus in close proximity to the brain. This may promote heat conduction from the probe and facilitate tissue heating by absorption due to the smaller insonated volume. Nonetheless, it illustrates the importance of temperature evaluation in monitoring protocols.

Intracranial hemorrhage as a side effect of therapeutic ultrasound is of particular interest. The clinical studies on sonothrombolysis using diagnostic Doppler or duplex devices show the potential benefits of sonothrombolysis for patients with intracranial arterial occlusion. In the CLOTBUST trial (using Doppler), no difference in the rate of symptomatic hemorrhage was detected between ultrasound treated and control patients (Alexandrov *et al*, 2004). Eggers *et al* (2008) (TCCS) found a trend toward an increased rate of symptomatic bleeding. Molina *et al* (2006) (Doppler), who added the contrast agent Levovist to the treatment protocol, and Perren *et al* (2008) (TCCS with SonoVue) did not detect differences in the incidence of intracranial hemorrhage. However, the number of patients included in these studies does not allow definite conclusions on the safety profile of contrast-enhanced sonothrombolysis. Our animal data support that microbubble-enhanced TCCS is safe with regard to the occurrence of intracranial hemorrhage. One of 25 animals treated with CEUS and rt-PA had intracerebral hemorrhage, without space-occupying effect and without clinical deterioration. Nonetheless, the limitations of these findings have to be acknowledged. Rats are generally viewed to display less bleeding complications in fibrinolytic treatment than humans. This is in contrast to earlier results of our study group and results by Saguchi *et al*, who detected significant rates of hemorrhage in rat models of ischemic stroke, pointing toward the utility of animal models for detection of bleeding complications (Nedelmann *et al*, 2008; Saguchi *et al*, 2008). Nonetheless, as hemorrhage is one major concern in therapeutic ultrasound trials (Daffertshofer *et al*, 2005), future trials will have to address this issue very carefully.

In conclusion, this study shows that extended CEUS application in combination with rt-PA not only is safe in the situation of reperfusion but displays beneficial effects on the level of the cerebral microvasculature resulting in reversal of flow obstruction and in a decrease of ischemic lesion volume and edema formation. We hereby show that sonothrombolytic treatment is not limited to recanalization of arterial main stem occlusion. This study supports the importance of larger clinical trials investigating therapeutic effects and safety of microbubble-enhanced ultrasound in acute cerebral artery occlusion.

Conflict of interest

The authors declare no conflict of interest.

References

Alexandrov AV, Molina CA, Grotta JC, Garami Z, Ford SR, Alvarez-Sabin J, Montaner J, Saqqur M, Demchuk AM, Moye LA, Hill MD, Wojner AW (2004) Ultrasound-enhanced systemic thrombolysis for acute ischemic stroke. *N Engl J Med* 351:2170–8

Allendoerfer J, Goertler M, von Reutern GM (2006) Prognostic relevance of ultra-early Doppler sonography in acute ischaemic stroke: a prospective multicentre study. *Lancet Neurol* 5:835–40

Daffertshofer M, Gass A, Ringleb P, Sitzer M, Sliwka U, Els T, Sedlaczek O, Koroshetz WJ, Hennerici MG (2005) Transcranial low-frequency ultrasound-mediated thrombolysis in brain ischemia: increased risk of hemorrhage with combined ultrasound and tissue plasminogen activator: results of a phase II clinical trial. *Stroke* 36:1441–6

Datta S, Coussios CC, Ammi AY, Mast TD, de Courten-Myers GM, Holland CK (2008) Ultrasound-enhanced thrombolysis using definity as a cavitation nucleation agent. *Ultrasound Med Biol* 34:1421–33

Dawson DA, Ruetzler CA, Hallenbeck JM (1997) Temporal impairment of microcirculatory perfusion following focal cerebral ischemia in the spontaneously hypertensive rat. *Brain Res* 749:200–8

Dirnagl U, Niwa K, Sixt G, Villringer A (1994) Cortical hypoperfusion after global forebrain ischemia in rats is not caused by microvascular leukocyte plugging. *Stroke* 25:1028–38

Eggers J, Konig IR, Koch B, Handler G, Seidel G (2008) Sonothrombolysis with transcranial color-coded sonography and recombinant tissue-type plasminogen activator in acute middle cerebral artery main stem occlusion: results from a randomized study. *Stroke* 39:1470–5

Fatar M, Stroick M, Griebe M, Alonso A, Kreisel S, Kern R, Hennerici M, Meairs S (2008) Effect of combined ultrasound and microbubbles treatment in an experimental model of cerebral ischemia. *Ultrasound Med Biol* 34:1414–20

Gerriets T, Stolz E, Walberer M, Muller C, Kluge A, Bachmann A, Fisher M, Kaps M, Bachmann G (2004) Noninvasive quantification of brain edema and the space-occupying effect in rat stroke models using magnetic resonance imaging. *Stroke* 35:566–71

Henning EC, Latour LL, Hallenbeck JM, Warach S (2008) Reperfusion-associated hemorrhagic transformation in SHR rats: evidence of symptomatic parenchymal hematoma. *Stroke* 39:3405–10

Langheinrich AC, Leithauser B, Greschus S, Von Gerlach S, Breithecker A, Matthias FR, Rau WS, Bohle RM (2004) Acute rat lung injury: feasibility of assessment with micro-CT. *Radiology* 233:165–71

Langheinrich AC, Michniewicz A, Bohle RM, Ritman EL (2007) Vasa vasorum neovascularization and lesion distribution among different vascular beds in ApoE−/−/LDL−/− double knockout mice. *Atherosclerosis* 191:73–81

Langheinrich AC, Yeniguen M, Ostendorf A, Marhoffer S, Dierkes C, von Gerlach S, Nedelmann M, Kampschulte M, Bachmann G, Stolz E, Gerriets T (2009) *In vitro* evaluation of the sinus sagittalis superior thrombosis model in the rat using 3D micro- and nanocomputed tomography. *Neuroradiology*; 18 November 2009; e-pub ahead of print

Molina CA, Ribo M, Rubiera M, Montaner J, Santamarina E, Delgado-Mederos R, Arenillas JF, Huertas R, Purroy F, Delgado P, Alvarez-Sabin J (2006) Microbubble administration accelerates clot lysis during continuous 2-MHz ultrasound monitoring in stroke patients treated with intravenous tissue plasminogen activator. *Stroke* 37:425–9

Nakagawa K, Ishibashi T, Matsushima M, Tanifuji Y, Amaki Y, Furuhata H (2007) Does long-term continuous transcranial Doppler monitoring require a pause for safer use? *Cerebrovasc Dis* 24:27–34

Nedelmann M, Wilhelm-Schwenkmezger T, Alessandri B, Heimann A, Schneider F, Eicke BM, Dieterich M, Kempski O (2007) Cerebral embolic ischemia in rats: correlation of stroke severity and functional deficit as important outcome parameter. *Brain Res* 1130:188–96

Nedelmann M, Reuter P, Walberer M, Sommer C, Alessandri B, Schiel D, Ritschel N, Kempski O, Kaps M, Mueller C, Bachmann G, Gerriets T (2008) Detrimental effects of 60 kHz sonothrombolysis in rats with middle cerebral artery occlusion. *Ultrasound Med Biol* 34:2019–27

Nedelmann M, Stolz E, Gerriets T, Baumgartner RW, Malferrari G, Seidel G, Kaps M (2009) Consensus recommendations for transcranial color-coded duplex sonography for the assessment of intracranial arteries in clinical trials on acute stroke. *Stroke* 40:3238–44

Okada Y, Copeland BR, Fitridge R, Koziol JA, del Zoppo GJ (1994) Fibrin contributes to microvascular obstructions and parenchymal changes during early focal cerebral ischemia and reperfusion. *Stroke* 25:1847–53

Perren F, Loulidi J, Graves R, Yilmaz H, Rufenacht D, Landis T, Sztajzel R (2006) Combined IV-intra-arterial thrombolysis: a color-coded duplex pilot study. *Neurology* 67:324–6

Perren F, Loulidi J, Poglia D, Landis T, Sztajzel R (2008) Microbubble potentiated transcranial duplex ultrasound enhances IV thrombolysis in acute stroke. *J Thromb Thrombolysis* 25:219–23

Pfeuffer J, Adriany G, Shmuel A, Yacoub E, Van De Moortele PF, Hu X, Ugurbil K (2002) Perfusion-based high-resolution functional imaging in the human brain at 7 Tesla. *Magn Reson Med* 47:903–11

Saguchi T, Onoue H, Urashima M, Ishibashi T, Abe T, Furuhata H (2008) Effective and safe conditions of low-frequency transcranial ultrasonic thrombolysis for acute ischemic stroke: neurologic and histologic evaluation in a rat middle cerebral artery stroke model. *Stroke* 39:1007–11

Schlosser HG, Doepp F, Nolte CH, Brock M, Schreiber SJ (2009) Does routine transcranial duplex ultrasound heat up the patient brain? *Ultraschall Med* 30:37–41

Siegel RJ, Suchkova VN, Miyamoto T, Luo H, Baggs RB, Neuman Y, Horzewski M, Suorsa V, Kobal S, Thompson T, Echt D, Francis CW (2004) Ultrasound energy improves myocardial perfusion in the presence of coronary occlusion. *J Am Coll Cardiol* 44:1454–8

Suchkova VN, Baggs RB, Sahni SK, Francis CW (2002) Ultrasound improves tissue perfusion in ischemic tissue through a nitric oxide dependent mechanism. *Thromb Haemost* 88:865–70

Thomalla G, Sobesky J, Kohrmann M, Fiebach JB, Fiehler J, Zaro Weber O, Kruetzelmann A, Kucinski T, Rosenkranz M, Rother J, Schellinger PD (2007) Two tales: hemorrhagic transformation but not parenchymal hemorrhage after thrombolysis is related to severity and duration of ischemia: MRI study of acute stroke patients treated with intravenous tissue plasminogen activator within 6 hours. *Stroke* 38:313–8

Todd NV, Picozzi P, Crockard HA, Russell RR (1986) Reperfusion after cerebral ischemia: influence of duration of ischemia. *Stroke* 17:460–6

Wunderlich MT, Goertler M, Postert T, Schmitt E, Seidel G, Gahn G, Samii C, Stolz E (2007) Recanalization after intravenous thrombolysis: does a recanalization time window exist? *Neurology* 68:1364–8